



POLITECNICO
MILANO 1863

SCUOLA DI INGEGNERIA INDUSTRIALE
E DELL'INFORMAZIONE

EXECUTIVE SUMMARY OF THE THESIS

Multislit collimator characterization and dosimetry measurements for microbeam radiation therapy applications at the ESRF - ID17 Biomedical beamline

LAUREA MAGISTRALE IN PHYSICS ENGINEERING - INGEGNERIA FISICA

Author: LUCIA MALUCELLI

Advisor: PROF. MARCO MORETTI

Co-advisor: DR. PAOLO PELLICOLI

Academic year: 2022-2023

1. Introduction

Microbeam radiation therapy (MRT) is an innovative radiation therapy technique developed around the spatial fractionation of the radiation field, to reduce radiation-induced side effect. MRT is based on the *Dose Volume Effect*, a phenomenon for which healthy tissues better tolerate high radiation if it is confined in micrometric volume. For the first time in 1990s microbeams were used in pre-clinical studies [2]. In MRT, spatial dose-fractionation is defined at micrometric scale. Fields are characterized by an array of planar microbeams 25-100 μm wide and a center-to-center (c-t-c) distance of 100-400 μm . Nowadays, the most common geometry of microbeams is of 50 μm wide beams, spaced by 400 μm pitch. The result is a spatial modulation of the delivered dose characterized by a peak dose (long the microbeam path) that can be up to some hundreds of Gy, and valley dose (between adjacent peaks) where dose is deposited following radiation scattering events in the irradiated volume. Valley dose is typically kept below the limit established for conventional radiotherapy to reduce side effect.

The development of MRT programs was possible thanks to the realization of high-energy Synchrotron Radiation sources capable of producing X-ray radiation that fulfills the requirements needed for MRT studies.

Nowadays MRT is in pre-clinical development in a small number of synchrotrons that present a beamline able to generate microbeams: the ID17 Biomedical beamline of the European Synchrotron Radiation Facility (ESRF) in Grenoble (France) and the Imaging and Medical beamline (IMBL) of the Australian Synchrotron (ANSTO) in Melbourne (Australia) are the most active laboratories in the MRT field.

The spatial fractionation of the homogeneous X-ray beam delivered by the wiggler device installed along the synchrotron storage ring is achieved by placing a multislit collimator (MSC) in front of the target. The MSC is a metal-based component machined to create a regular pattern of equidistant aperture with identical width. Nowadays, MSCs of fixed geometry are often preferred to variable apertures ones because easier to align and more reliable during experiment. Typically made of a tungsten-based alloy, MSCs are created from a single metal

block or assembling individual blades for obtaining the desired width and spacing of microbeam array.

Figure 1 shows the technical drawing of one of the MSCs available at ID17.

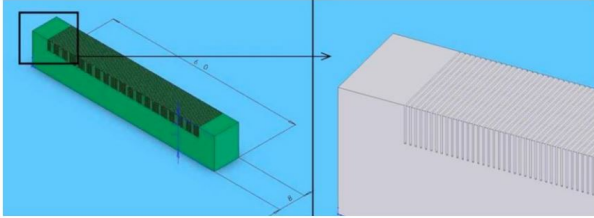


Figure 1: Technical drawing of a single block MSC available at the ID17 beamline [1].

The MSC available at the ID17 beamline since 2009 is the CF-H25S+ (CF) MSC, characterized by apertures with nominal width of $50\ \mu\text{m}$ and a c-t-c distance of $400\ \mu\text{m}$.

To perform MRT irradiation, the control on the radiation delivered to the target is essential, as in all RT techniques. Several dosimetry protocols specific for MRT have been developed, but measured valley doses are often up to 10-30% bigger than simulated ones, a difference too high to match the agreement typically needed for RT applications. For this reason, a new MSC has been realized in Densimet 185 material, a more recent tungsten-based alloy with properties closer to those of the pure tungsten. The Densimet MSC is expected of reducing the transmitted radiation through the MSC blades and thus the delivered valley dose to the target [4].

The aim of this work is to characterize the new MSC and quantify the improvements with respect to the CF MSC. The work includes measurements of the transmission spectra and experimental dosimetry together with Monte Carlo simulations of the delivered dose to the target phantom.

2. Material and Methods

2.1. Experimental setup at the ESRF ID17 Biomedical beamline

The study was done at the ID17 biomedical beamline of the ESRF. The beamline was designed with the aim of supporting innovative works in radiation therapy and medical imaging. The synchrotron radiation source at the ID17 is

a wiggler of 1.5 m length and a magnetic field of 1.6 T at a gap of 24.8 mm. Before reaching the target, placed around 40.5 m from the source point, the beam passes through two couple of motorized slits, for the first field size definition, and a combination of filters that allow to cut photon energies below 50 keV, non-effective for microbeam treatments. Different combinations of attenuators allow to change the configuration of spectra profiles and intensities. Two ionization chambers (IC1 and IC2) can be moved inside the beam for monitoring purposes. The final beam height is defined by one of four vertical apertures with fixed dimension ($51\ \mu\text{m}$, $102\ \mu\text{m}$, $520\ \mu\text{m}$ and $795\ \mu\text{m}$) centered with the center of the beam. A couple of motorized horizontal slits can be moved inside the beam to precisely define a beam width below 1 mm. The maximum dimension of the beam reaching the target is of $2\ \text{mm} \times 35\ \text{mm}$, too small to directly irradiate a target with a vertical extension higher than 2 mm. In order to overcome this limitation a scanning technique is used: the sample is placed on a kappa-type goniometer and it is vertically translated at constant speed through the photon beam. The vertical movement range of the goniometer is of approximately 14 cm.

2.2. Characterization of the multislit collimator

The two MSCs used at ID17 for microbeams generation are the CF MSC, made of CF-H25S+, a metal alloy of tungsten carbide (WC, 90.3 wt%), cobalt (Co, 8.5 wt%), vanadium carbide and chromium carbide ($\text{VC}+\text{Cr}_3\text{C}_2$, 1.2 wt%), with a density of $14.55\ \text{g}/\text{cm}^3$, and the Densimet MSC, made of a metal alloy of tungsten (W, 96.97 wt%), nickel (Ni, 2.02 wt%) and iron (Fe, 1.01 wt%) and with a nominal density of $18.54\ \text{g}/\text{cm}^3$. Both MSCs are made of a 8 mm thick single copper block, hosting 125 individual blades fitted to obtain the desired aperture width and spacing of the microbeams array. This mechanical design was used because wire-cutting techniques are not precise enough for obtaining apertures less than $100\ \mu\text{m}$ from a single metal block.

After a cleaning process of the apertures, necessary to verify that small residues from the machining procedure are not stuck between blades, the regularity of the aperture width and peri-

odicity of both MSCs is checked using the synchrotron beam. Defining a beam width of 15-20 μm and aligning the apertures with the beam, the profile of each single microbeam, i.e. the radiation profile defined by each MSC aperture, is obtained by an horizontal scans of the MSC. The motor is moved for a range of 52 mm, by steps of 5 μm (motor resolution), thus obtaining a set of 10401 points per scan.

To calculate the FWHM of each microbeam and the c-t-c distance between microbeams a Matlab code is developed.

2.3. Radiation transmitted through the multislit collimator blades

The final X-ray spectrum impinging on the MSC is calculated using the OrAnge SYnchrotron Suite (OASYS) platform, as described in the work of Di Manici [5]. In the present work two spectra configurations are considered: the *conventional spectrum*, used in most pre-clinical experiments, has the maximum intensity of 16000 Gy/s and a mean energy of 103 keV; the *clinical spectrum*, with a higher mean energy of 120 keV defined by means of thicker attenuators, is used when irradiation in a clinical scenario are necessary to be more penetrating the matter, reducing dose delivery in dense biological tissues such as bones. Figure 1 shows the spectrum profiles of the conventional and clinical spectrum used.

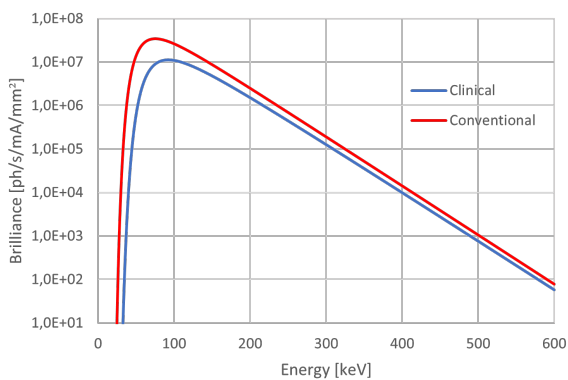


Figure 2: Spectrum intensity profile corresponding to the conventional and clinical spectrum used at the ESRF-ID17 beamline for MRT experiments.

While the X-ray beam arriving on the MSC in correspondence of the collimator aperture passes undisturbed and reaches the target, the radiation impinging on the MSC blades is mostly

absorbed inside the collimator. However, a small part of radiation is transmitted through the MSC blades and it can be calculated starting from the mass attenuation coefficients taken from the NIST database (Hubbell and Seltzer, 1996) and applying the Lambert-Beer law. Multiplying the transmittance with the X-ray spectrum for both clinical and conventional configuration, the transmitted spectrum through the blades of the MSCs is calculated. The transmitted spectra is calculated with MC approach as well to validate the spectrum model used in simulations of dose delivery.

2.4. Dosimetry validation

A PTW microDiamond detector (PTW, Freiburg, Germany) is used to measure the radiation transmitted by a small beamlet (narrower than a single MSC blade) impinging on a single blade of the MSCs. This solid-state detector is aligned in edge-on configuration along the beam path to profit of the active volume made of a synthetic single crystal diamond with a cylindrical shape only 1 μm thickness.

Radiochromic film are then used for measuring the two-dimensional dose distribution produced during an irradiation of an arrays of microbeams. The films used in this study are the GAFchromic EBT3 films, produced by Ashland company.

Film dosimetry in air is performed to assess the difference of the valley dose reaching the surface of the target depending on the MSC used. The conventional and the clinical spectrum are used and three field size are considered: $20 \times 20 \text{ mm}^2$, $10 \times 10 \text{ mm}^2$ and $5 \times 5 \text{ mm}^2$. Three films are irradiated for each configuration of spectrum, MSC and field size used. For the valley dose evaluation, the four central valleys of each field are considered.

To quantify the variation of the valley dose due to the use of the two different MSCs in a more realistic conditions of bigger targets, films are irradiated inside a water-equivalent $18 \times 18 \times 18 \text{ cm}^3$ phantom at the depth of 3 mm, 5 mm, 10 mm and 20 mm. In this case, only the clinical spectrum is used and the same three different field size. Two films are irradiated for each configuration and the dose values of four central valleys are considered for each sample.

For the films analysis, an optical microscope is

used to scan and digitalized the samples and, by means of a Matlab program inhouse developed at the beamline [3], dose profiles are obtained. MC simulations, based on Geant4 toolkit, is used to calculate the valley dose inside the phantom reproducing the setup used for film dosimetry. The comparison between simulated and measured dose differences when using the two MSCs is then possible.

3. Results and discussion

3.1. Apertures dimension and spacing periodicity of the MSCs

The measurement of the FWHM and of the c-t-c distance between consecutive apertures of the CF and the Densimet MSC shows good agreement with the nominal values with small error due to uncertainties in the measurement or possible misalignment of the blades, that could cause different amount of radiation passing through each single apertures depending on its alignment with respect to the beam.

For the CF MSC the FWHM, shown in figure 3, is around $52 \mu\text{m}$ in the central part while it drops down to around $47 \mu\text{m}$ at the edges. The average value of the FWHM is $49.78 \mu\text{m}$, really close to the nominal value of $50 \mu\text{m}$, with a standard deviation of $\pm 1.43 \mu\text{m}$ (2σ). The c-t-c distance, shown in figure 4, oscillates between $397 \mu\text{m}$ to $403 \mu\text{m}$. The average c-t-c distance is $399.87 \mu\text{m}$ with a variation of $\pm 1.66 \mu\text{m}$ (2σ), very close to the nominal value of $400 \mu\text{m}$.

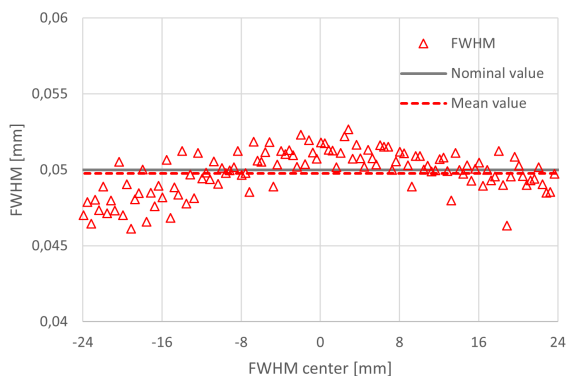


Figure 3: Plot of the FWHM measured for each aperture of the CF MSC.

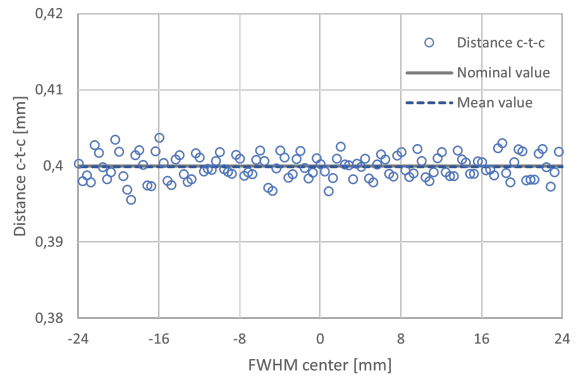


Figure 4: Center-to-center distance between consecutive apertures for the CF MSC.

The FWHM of Densimet MSC, shown in figure 5, is almost $50 \mu\text{m} \pm 1.5 \mu\text{m}$ for motor positions between -8 and 24 mm, but around motor position -15 mm the apertures width is greatly reduced, down to around $45 \mu\text{m} \pm 1.5 \mu\text{m}$. This suggests the presence of blades misalignment, confirmed by the results obtained making a new scan of the Densimet MSC, after having redefined the aligned of three apertures located at position -15 mm: the FWHM distribution of $50 \mu\text{m}$ is observed around -15 mm motor position but decreases at around $46 \mu\text{m}$ elsewhere.

The c-t-c distance remain constant for both alignment angles with an average value of $399.85 \mu\text{m} \pm 2.24 \mu\text{m}$ (2σ), almost equivalent to the nominal value of $400 \mu\text{m}$, with a c-t-c values distribution equivalent to the CF MSC presented in Figure 4.

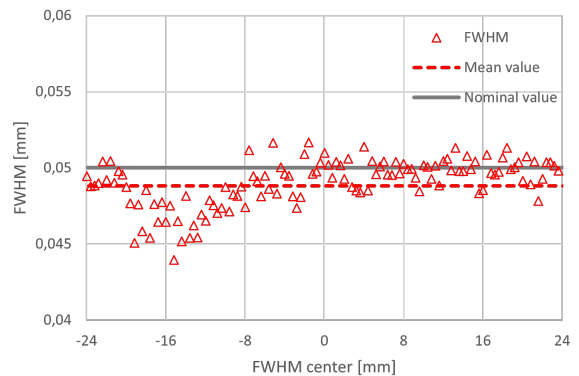


Figure 5: Plot of the FWHM measured for each aperture of the Densimet MSC with the beam aligned with the three central apertures.

3.2. Radiation transmission through the multislit collimator blades

Figure 6 shows the transmittance as a function of the photon energy for the CF and the Densimet MSC, compared to the case of an ideal MSC made of pure tungsten.

The transmittance of the Densimet MSC is significantly reduced compared to the CF MSC especially in the 200-300 keV range.

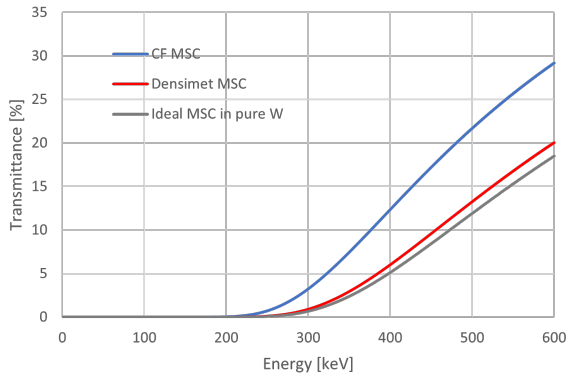


Figure 6: Theoretical X-ray transmittance distribution as a function of the photon energy for the CF and the Densimet MSC compared with an ideal MSC made of pure tungsten. Calculation done on the base of the NIST database.

Figure 7 shows the expected X-ray transmitted spectra by the CF and the Densimet MSC, obtained by multiplying the clinical spectrum profile by the transmittance of both MSC. The MC simulated transmitted spectra are in perfect agreement with the calculated spectra.

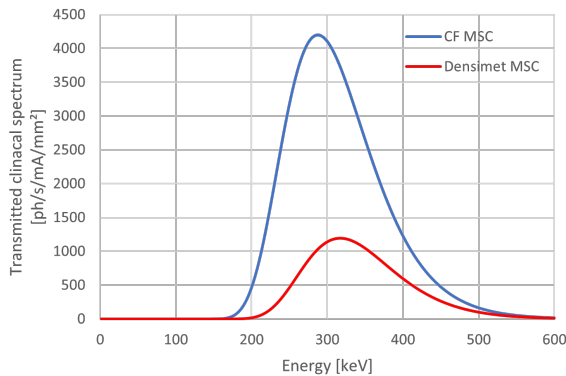


Figure 7: X-ray transmitted spectra by the CF MSC (blue curves) and the Densimet MSC (red curves) considering the clinical spectrum. Profiles calculated starting from mass attenuation coefficients of the NIST database.

Using the Densimet MSC the transmitted radiation decreases with respect to the spectrum transmitted by the CF MSC of the 70%.

3.3. Dosimetry validation

For the measurement with the microdiamond detector of the different transmitted radiation by both MSCs using the clinical spectrum, the measured transmitted dose rate is around 0.11 mGy/s/mA for the CF MSC and 0.04 mGy/s/mA for the Densimet MSC with a negligible variation between the central 6 blades. The % difference of the transmitted radiation measured between the two collimators is 65% less when using the Densimet MSC with respect to the CF MSC. This value is in close agreement with the theoretical value of 70% calculated in section 3.2.

Film irradiated in air with an array of microbeams represents a more complex scenario where the presence of several intense microbeams brings a significant contribution to the valley dose. The interaction of the radiation with the inner walls of the MSCs may generate an undesired contribution of scattered radiation reaching the valley region, modifying the rounded profile of valleys dose. A clear difference between clean and distorted valley dose profiles is shown in figure 8, obtained from the CF and the Densimet MSC. Overall, the CF MSC introduces more artefacts in the valley dose profiles.

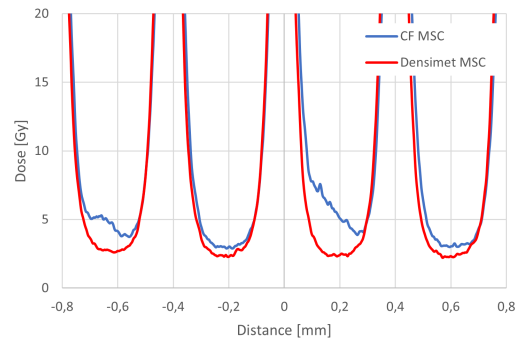


Figure 8: Detail of valley dose profile measured with radiochromic films using the CF MSC (blue line) and Densimet MSC (black line).

Considering different field sizes the average valley dose slightly decreases with the decrease of the field dimension. Indeed for larger fields the contribution of the scattered radiation inside the

target (the film only in this case) increases. Using the Densimet MSC an average valley doses reduction of 33/35% is measured. Using an entire array of microbeam, the biggest contribution to the valley dose is related to the scattered photons. This contribution is added on top to the weaker difference of the radiation transmitted by the MSC blades. Overall, a clear difference between the dose delivered by the two different collimators is observed, with the Densimet MSC more capable in defining a cleaner array of microbeam. Table 1 summarizes the result of the film dosimetry in air.

| Field size mm^2 | Total valley dose [Gy] | | %diff |
|----------------------|------------------------|----------|--------|
| | CF MSC | Densimet | |
| 20x20 | 4.2±0.9 | 2.8±0.2 | -33.84 |
| 10x10 | 3.9±0.9 | 2.6±0.2 | -33.78 |
| 5x5 | 3.9±0.9 | 2.5±0.1 | -35.99 |

Table 1: Valley dose measurements by film dosimetry in air using the clinical spectrum and both, CF and Densimet, MSCs.

The study of depth dose profile delivered in MRT configuration in the water equivalent phantom provides the final valley dose difference when the two MSCs are used in a more conventional irradiation scenario. Figure 9 shows the depth dose profile of the valley dose for a 5×5

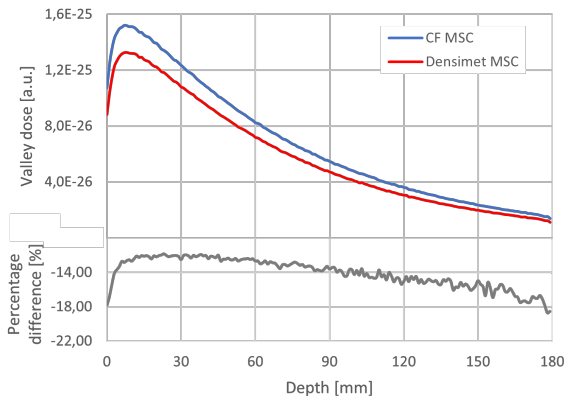


Figure 9: On top, MC simulation of valley depth dose profile obtained for the CF and Densimet MSC for a 5×5 mm^2 field size and clinical spectrum. At the bottom, percentage difference of the valley dose obtained with the Densimet MSC with respect to the CF MSC.

mm^2 array of microbeams simulated using the clinical spectrum and both CF and Densimet collimators, together with the percentage difference between the two profiles. The differences are up to -18% at the phantom surface and between -13% and -16% inside the cubic phantom. For a 10×10 mm^2 and a 20×20 mm^2 field size a similar behavior is obtained with reduced differences due to the increase of the field size. Table 2 and 3 show the results obtained from film dosimetry inside the phantom for the 20×20 mm^2 and the 5×5 mm^2 field size, respectively, comparing the CF and the Densimet MSC case, together with the measured and the simulated % difference. Similar results are obtained for the 10×10 mm^2 .

| Depth [mm] | Average valley dose [Gy] | | %diff | |
|------------|--------------------------|----------|--------|-------|
| | CF | Densimet | Film | MC |
| 3 | 2.2±0.1 | 1.9±0.1 | -12.83 | -6.78 |
| 5 | 2.4±0.0 | 2.2±0.1 | -9.49 | -5.79 |
| 10 | 2.6±0.1 | 2.4±0.0 | -9.25 | -5.34 |
| 20 | 2.8±0.1 | 2.5±0.1 | -9.21 | -4.48 |

Table 2: valley dose measurements by film dosimetry in water-equivalent phantom at different depth for a 20×20 mm^2 field using the CF MSC and the Densimet MSC, together with measured and the simulated % differences.

| Depth [mm] | Average valley dose [Gy] | | %diff | |
|------------|--------------------------|----------|--------|--------|
| | CF | Densimet | Film | MC |
| 3 | 2.1±0.0 | 1.8±0.1 | -15.27 | -14.12 |
| 5 | 2.2±0.1 | 1.9±0.1 | -14.77 | -13.32 |
| 10 | 2.3±0.1 | 1.9±0.1 | -16.58 | -12.70 |
| 20 | 2.1±0.0 | 1.8±0.1 | -12.26 | -12.20 |

Table 3: valley dose measurements by film dosimetry in water-equivalent phantom at different depth for a 5×5 mm^2 field using the CF MSC and the Densimet MSC, together with measured and the simulated % differences.

Comparing measured valley dose differences, the average % difference among the different depth

considered using the Densimet MSC instead of the CF MSC goes from around -10% for a $20 \times 20 \text{ mm}^2$ field to around -15% for a $5 \times 5 \text{ mm}^2$ field. Same trend is obtained with MC simulations: the % difference goes from -5% with a $20 \times 20 \text{ mm}^2$ field to around -13% with a $5 \times 5 \text{ mm}^2$ field. Due to the augmented scattered radiation contribution inside the cubic phantom, the dose differences between valleys defined by the CF or Densimet MSC is decreased with respect to the case observed of films irradiated in air. In addition bigger it is the field size, stronger is the contribution of the scattering events happening inside the target making overall less distinguishable the contribution of the transmitted or scattered radiation inside the MSCs and reaching the sample. Film dosimetry and MC simulations in the water-equivalent phantom show similar results with differences probably due to the too simple model of the MSC realized for MC simulations where the blades misalignment is not considered.

Overall, the study confirms the improvement obtained when using the Densimet MSC for MRT experiments, with less radiation delivered into the valley regions.

4. Conclusions

The development of MRT opens new perspectives in the research for cancer defeating with the spatial fractionation of the irradiation field at micrometric scale. When X-ray radiation sources are used for spatial fractionated radiotherapy approaches the use of a MSC is necessary and a full understanding and characterization of the interaction of the radiation with this component is essential to control in a reliable way the irradiation process. The aim of the study is to characterize a new MSC made of Densimet material and compare it with the CF-H25S+ MSC already used at the ESRF-ID17 biomedical beamline.

The radiation transmitted through the MSC blades is measured with a PTW microdiamond detector obtaining a radiation reduction of the 65% when using the Densimet MSC rather than the CF MSC, in great agreement with the theoretical value of 70% calculated using NIST's database or MC simulations.

The delivered valley dose to the target surface is measured by radiochromic films irradiated in air

and a reduction of -30% valley dose is observed when using the new MSC. When valley doses are measured inside a water-equivalent phantom, -10% valley dose for a $20 \times 20 \text{ mm}^2$ field and -15% for a $5 \times 5 \text{ mm}^2$ is observed when using the new MSC, with MC simulations providing close values to the measured ones.

The Densimet MSC is able to improve the reliability of MRT experiments by defining cleaner arrays of microbeams and reducing the dose delivered in valley regions where doses must be reduced as much as possible when irradiation biological tissues.

This study presents a solid approach for the characterization of MSCs and can be considered the starting point for further study and development of MRT technique connected to the use of MSCs.

5. Acknowledgements

I would like to thank my supervisor Dr. Paolo Pellicoli for the precious help during my internship at the ESRF and in developing the project, and Dr. Liam Day for the help with Monte Carlo simulations.

References

- [1] E.Bräuer-Krisch et al. New technology enable high precision multislit collimators for microbeam radiation therapy. *Review of scientific instruments*, 80, 2009.
- [2] J.A.Laissue et al. The weanling piglet cerebellum: a surrogate for tolerance to mrt (microbeam radiation therapy) in pediatric neuro-oncology. *Penetrating Radiation Systems and Applications III*, 4508, 2001.
- [3] P.Pellicoli et al. High resolution radiochromic film dosimetry: Comparison of a microdensitometer and an optical microscope. *European Journal of Medical Physics*, 2019.
- [4] P.Pellicoli et al. Study of the x-ray radiation interaction with a multislit collimator for the creation of microbeams in radiation therapy. *Journal of Synchrotron Radiation*, 2020.
- [5] I. Di Manici. Synchrotron x-ray spectra characterization for radiation therapy applications at the esrf - id17 biomedical beamline. Master's thesis, Politecnico di Milano, 2021.